ELSEVIER

Materials Science and Engineering A262 (1999) 9–15

MATERIALS SCIENCE & ENGINEERING A

Characterization of SiC_p/2024 aluminum alloy composites prepared by mechanical processing in a low energy ball mill

R. Angers, M.R. Krishnadev, R. Tremblay, J.-F. Corriveau [1], D. Dubé *

Department of Mining and Metallurgy, Université Laval, Québec G1K 7P4, Canada

Received 27 June 1998; received in revised form 6 October 1998

Abstract

In the present work, SiC_p/2024 composite powders were produced by low energy ball milling a mixture of centrifugally atomized 2024 particles and β-SiC reinforcements having a size range between 2 and 6 μm. The experimental parameters studied were the milling time (between 1 and 24 h) and the volume proportion of β-SiC in the starting powder mixture (between 5 and 35%). These SiC_p/2024 composite powders were consolidated by hot extrusion using optimized processing parameters. The microstructure of the extruded composites showed a uniform distribution of β-SiC particles in the 2024 aluminum matrix. Moreover, the mechanical properties (yield strength and Young's modulus) improved with the SiC content although some reduction in ductility was observed. © 1999 Elsevier Science S.A. All rights reserved.

Keywords: Low energy ball milling; Optimized processing parameters; Yield strength

1. Introduction

For more than two decades, aluminum-matrix composites have been made by different methods including casting [1–9], spray atomization and codeposition [9,10], pressure-infiltration of porous ceramic preforms [11], and powder metallurgy techniques like densification of mixtures of metal and ceramic powders [12–17], or of composite powders made by mechanical processing [13,18–34]. The mechanical properties of these composites are influenced significantly by the quantity and mode of distribution of the reinforcements and also by the nature of the interfaces between the reinforcements and the matrix. In this context, the use of mechanically processed composite powders for producing sound aluminum matrix composites or other metal-matrix composites (MMCs) should be considered as a very promising and commercially viable technique since the starting composite powders are characterized by a uniform distribution of reinforcement particles [2,8,29,32]. Also this low temperature solid-state process eliminates reactions between the reinforcement particles and the matrix which are indeed an important problem with methods involving molten metal [4,6]. However mechanical processing is only suitable for composites reinforced with small particles since whiskers and fibers fracture during mechanical processing [30,33]. The fabrication of MMCs by mechanical processing is more attractive technologically and economically when a low energy conventional ball mill is used instead of a high energy attritor as it is the common practice [23–26,28,32,34]. For this reason, in the present study, Al-matrix composite powders were produced with a low energy ball mill. These composite powders were consolidated by hot extrusion and the microstructure and mechanical properties of the composite specimens were evaluated. The results clearly show that homogeneous microstructures and excellent mechanical properties can be obtained by this method.

* Corresponding author. Tel.: +1-4186562131; fax: +1-4186565343; e-mail: ddube@gmn.ulaval.ca.

[1] Present address: Cegep de Trois-Rivières, Trois-Rivières, Québec, Canada G9A 5E6.

PII: S0921-5093(98)01030-2

2. Experimental procedure

2.1. Mechanical processing of composite powders

A conventional 29 cm diameter by 15 cm long cylindrical cast iron ball mill with an internal volume of 10000 cm^3 was used for this study. It was rotated at 6.28 rad s^{-1} (60 rpm) for all experiments which corresponds to 77% of its critical rotational speed (8.2 rad s^{-1}). Approximately 10% of the internal volume of the ball mill was filled with type 52100-bearing steel balls having a diameter of 19 mm, a hardness of 65 Rockwell 'C' and weighing 28 g each. The internal surface of the ball mill was lined with a 2024 alloy sheet to prevent contamination of the powder by cast iron. The vacuum tight ball mill was evacuated and backfilled with argon prior to mechanical processing to reduce oxidation to a minimum.

The starting powder mixture was composed of gas atomized 2024 aluminum powder[2] ($d_{av} = 110$ μm) and angular β-SiC powder[3] with a narrow size distribution between 2 and 6 μm ($d_{av} = 3$ μm). Parameters that were maintained constant during all experiments were the ball mill angular velocity (6.28 rad s^{-1}), the number of steel balls (292), the internal atmosphere in the cylinder (argon), the mass of 2024 powder in the mixture (60 g) and the size of SiC reinforcement particles. Parameters that were varied were the milling time (1–24 h) and the proportion of SiC_p in the starting powder mixture (5–35 vol.%). No process control agent (PCA) was used during this work.

2.2. Fabrication of composite specimens

The SiC_p/2024 composite powders used to prepare the extruded rods were ball milled for 6 h. It was found by experience that this minimum milling time is required to produce a uniform distribution of SiC_p reinforcements within the 2024 aluminum matrix. Chemical analyses indicated that the effective volume proportions of SiC particles in the three powders produced were 7.4, 14.6 and 25.3%. A blank specimen without any reinforcement (only 2024 powder) was also produced for comparison purposes.

The composite powder was first consolidated to 85–90% of the theoretical density by cold isostatic pressing at 270 MPa. The compacted preforms were placed in aluminum cans which were degassed under vacuum and sealed. These evacuated cans were then preheated to 500°C for 0.5 h and extruded in a die heated to 400°C. The transfer time between the furnace and the die was less than a few seconds. A graphite base lubricant was used to facilitate the extrusion. The extrusion ram speed was kept constant at 1 cm s^{-1} and the extrusion ratio was 17:1 which required an average pressure of about 250 MPa during extrusion. The extruded specimens were heat treated to T6 condition (solution heat treatment at 495°C for 1 h, water quench and artificial aging at 190°C for 12 h).

2.3. Microstructural and mechanical evaluation

Cylindrical tensile specimens with gauge diameter and gauge length of 4.1, and 16.3 mm, respectively, were machined from the extruded samples in accordance with ASTM B 557-94 standard [35]. Tensile tests were carried out at room temperature at a strain rate of 0.0001 s^{-1}. The microstructure of each specimen was examined by optical microscopy (OM) and scanning electron microscopy (SEM).

3. Results and discussion

3.1. Microstructure of SiC_p/2024 composite powders

The composite powders made by mechanical processing display a quite irregular shape (Fig. 1). Polished cross-sections of the powder containing 5 vol.% SiC_p are shown in Fig. 2 for different milling times up to 6 h. After short milling times, SiC_p reinforcement particles are found only at the periphery of the 2024 particles and as time increases they gradually penetrate into these particles. A uniform distribution of the reinforcements is obtained after about 6 h of mechanical processing. Tests made with different milling times up to 24 h showed that the distribution of SiC_p in the composite particles remains the same for all milling times between 6 and 24 h.

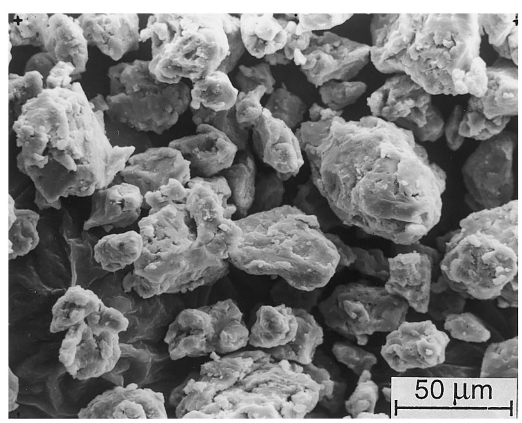

Fig. 1. Morphology of the SiC_p(5 vol.%)/2024 composite powder mechanically processed during 6 h (SEM).

[2] 93.6%Al, 4.2%Cu, 1.5%Mg, 0.7%Mn.

[3] Superior Graphite Co., Chicago, IL., Type HSC-0771, 96-98w/o SiC, 1.7w/o SiO2, 0.6w/o C (free), 0.2w/o N, < 0.03 w/o Si (free).

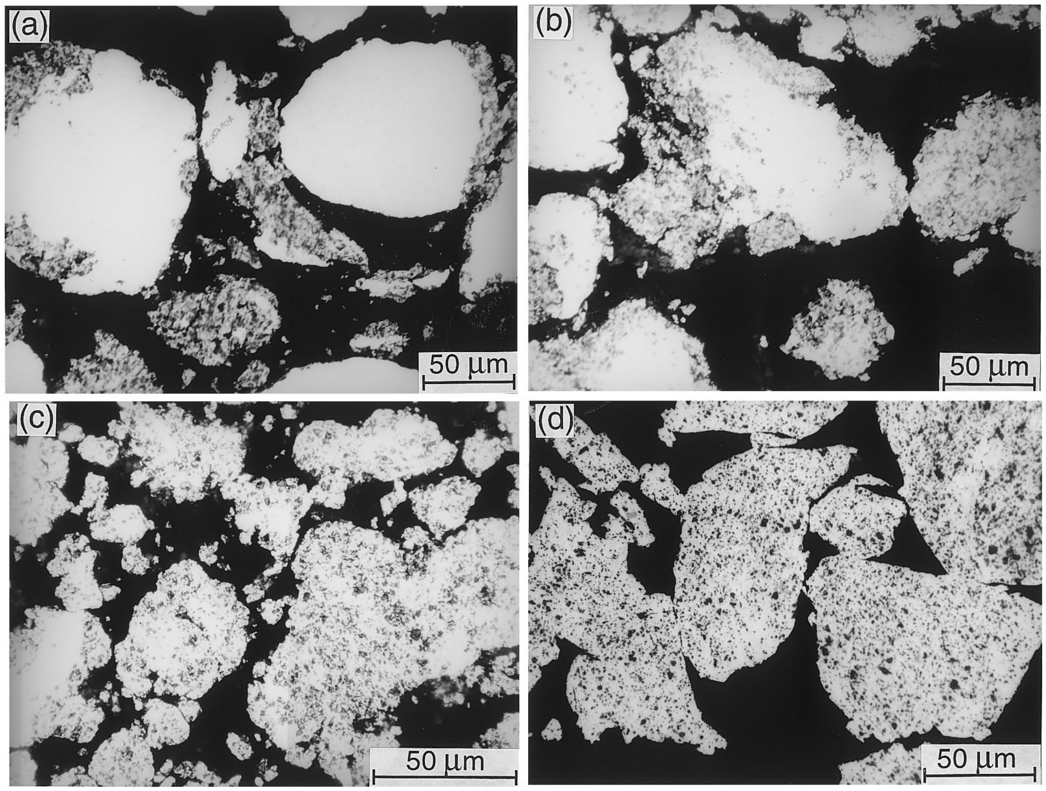

Fig. 2. Sections of the SiC_p(5 vol.%)/2024 composite particles mechanically processed during (a) 1 h, (b) 2 h, (c) 4 h and (d) 6 h. The SiC particle distribution in the composite powder is quite homogeneous after 6 h of milling (OM; unetched).

Polished sections of composite powders containing 5–35 vol.% SiC_p and milled for 6 h are shown in Fig. 3. It can be seen that the dispersion of SiC_p reinforcements in composite particles is uniform and does not depend significantly upon the SiC_p content. The composite powders with a high SiC_p content, e.g. 35 vol.%, appear fully saturated with SiC particles and a few clusters of these particles can be found which could have an adverse effect on the mechanical properties of finished parts [32,36,37]. Mechanical properties were not determined on specimens containing more than about 25 vol.% SiC particles.

A few mechanical processing experiments were also made with a starting mass of 2024 powder of 120 g instead of 60 g. It was found that with a larger quantity of starting powder, the necessary mechanical processing time increases for complete homogeneity. This effect was expected, and considering the random characteristics of the process, it can be anticipated that a change in other parameters of mechanical processing (such as the size of the ball mill) will also influence the final product [26,30].

3.2. Microstructure and mechanical properties of composite specimens

The microstructure of extruded rods containing 7.4, 14.6 and 25.3 vol.% SiC_p showed a homogeneous distribution of SiC particles and confirmed that a uniform particle distribution was originally obtained in the mechanically processed powder. The transverse and longitudinal cross-sections of extruded rod containing 14.6 vol.% SiC_p/2024 are shown in Fig. 4. These microstructures confirm that the SiC_p reinforcement distribution is spatially homogeneous which is imperative for isotropic properties. Only a few narrow bands with slightly different SiC_p densities were apparent in longitudinal cross-sections. The dispersion of SiC particles as viewed at high magnification (Fig. 5) is relatively uniform, showing few clustering. The 2024-T6 matrix showed equiaxed grains (average size $=5$ µm). Etching the aged rods in 0.5% HF revealed Al_2Cu precipitates smaller than 0.5 µm. No cracks or visible porosity were found after extrusion and heat treatment.

The mechanical properties measured by tensile testing are listed in Table 1 and compared to cast 2024 specimens and extruded 2024 powders. These results indicate that the Young's modulus increases steadily with the volume proportion of SiC_p. The rule of mixtures cannot be applied to determine the elastic modulus of such composites because it is only valid for composites reinforced with continuous fibers. However the elastic modulus of discontinuously reinforced com-

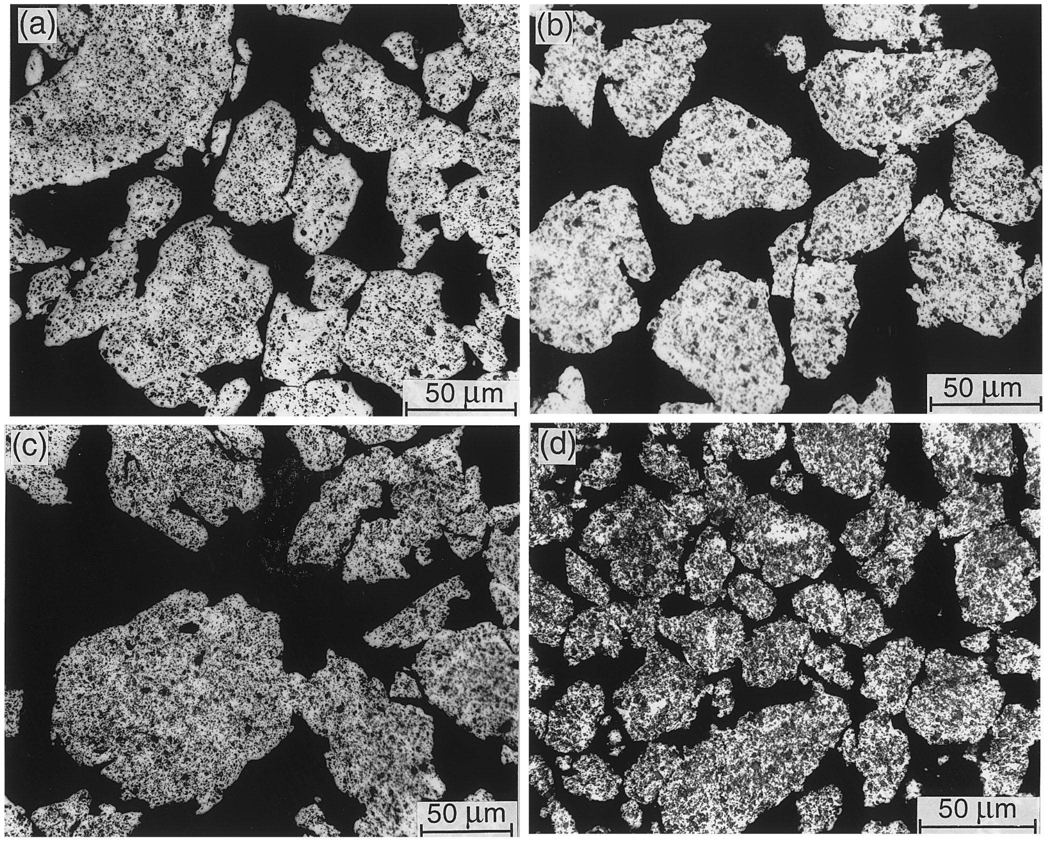

Fig. 3. Particle cross-sections showing the distribution of SiC reinforcement particles in the composite powders milled during 6h and containing (a) 5 vol.% SiC_p, (b)15 vol.% SiC_p, (c) 25 vol.% SiC_p and (d)35 vol.% SiC_p (OM; unetched).

posites E_c can be estimated using the Tsai–Halpin equation [38]:

$$E_c = E_m\ (1 + \zeta\eta V_p)/(1 - \eta V_p)$$

the parameter η being given by the following equation:

$$\eta = (E_p/E_m - 1)/(E_p/E_m + \zeta)$$

where E_m and E_p are the Young's moduli of the matrix, and SiC particles, respectively, V_p is the SiC volume fraction in the composite and ζ is a parameter related to the reinforcements which depends on boundary conditions between the SiC particles and the matrix. Young's modulus of the SiC particles and 2024 matrix introduced in calculations were $E_{SiC} = 450$ GPa and $E_{matrix} = 72$ GPa. The measured and predicted elastic moduli of composites are compared in Fig. 6 assuming a value of 2 for ζ in theoretical model [38]. The elastic modulus estimated from the rule of mixtures (isostrain condition) is shown only for comparison purposes. The experimental values appear to be well fitted by the Tsai–Halpin equation.

Yield strength and ultimate tensile strength are improved by the addition of SiC particles (Table 1). The yield strength of composites σ_{cy} can be compared to the theoretical strength using the following relation proposed by Nardone and Prewo [39]. It is based on a modified shear-lag model extended to the case of particulate composites:

$$\sigma_{cy} = \sigma_{my}\ \{[V_p(1 + S/2)] + [1 - V_p]\}$$

where σ_{my} is the yield strength of the matrix and S is the effective aspect ratio of the reinforcement. The measured and calculated yield strength (using $S = 1$, 2 and 4) are presented in Fig. 7. An effective aspect ratio $S = 4$ is required to give a satisfactory agreement with the measured yield strength. This effective aspect ratio is somewhat larger than suggested by visual observation of reinforcement particles, a ratio between 1 and 2 being more realistic for the SiC particles used in the present work. Similar observations were made by Jain et al. [17], who experimented with SiC_p/2124 composites produced by conventional powder metallurgy and extrusion methods and by Lagacé and Lloyd [2], who studied cast and extruded SiC_p/6061 composites. This discrepancy may be attributed to various factors not included in this model. One of these factors is the intrinsic strengthening of the matrix by increased dislocation density. According to Arsenault and Fisher [40], these dislocations are generated by high stresses produced by the low thermal expansion of the SiC particulates within the 2024 matrix. This higher density of dislocations also modifies the aging behavior, producing accelerated hardening [7,26,34,41,42]. Another explanation for this discrepancy is the restriction to the movement of dislocations by fine SiC particles (Orowan mechanism). Fine SiC particles are known to be produced by the incidental crushing of SiC particles during the ball milling of the composite powder [29,32]. Although no characterization of fine particles was carried out, it is believed that they can contribute to some strengthening of the matrix.

Table 1 indicates that the elongation of the composites is reduced by the addition of SiC particles. This general trend was also noted for many aluminum matrix composites produced by other methods [2,6,7,12,14,15,17]. The visual observation of the fractured surfaces showed that limited plastic deformation took place during tensile tests in agreement with the measured elongations. However, a magnified view of the fractured surface revealed that plastic deformation occurred in the 2024 matrix. The fractured surfaces of unreinforced 2024-T6 specimen reveal extensive dimpling typical of ductile ruptures (Fig. 8). By contrast, the ruptured face of 7.5% SiC_p/2024-T6 composites showed multiple elongated craters which were associated with larger SiC_p reinforcements indicating a high matrix-particle interface strength (Fig. 9a). These craters were surrounded by limited but well defined dimple structures, confirming that a partially ductile fracture took place (Fig. 9b). The presence of hard and non-ductile particles limited the deformation to a zone comprised between these particles and resulted in a globally small ductility. It was very difficult to find dimples at the fractured surface of composites containing more SiC_p reinforcements.

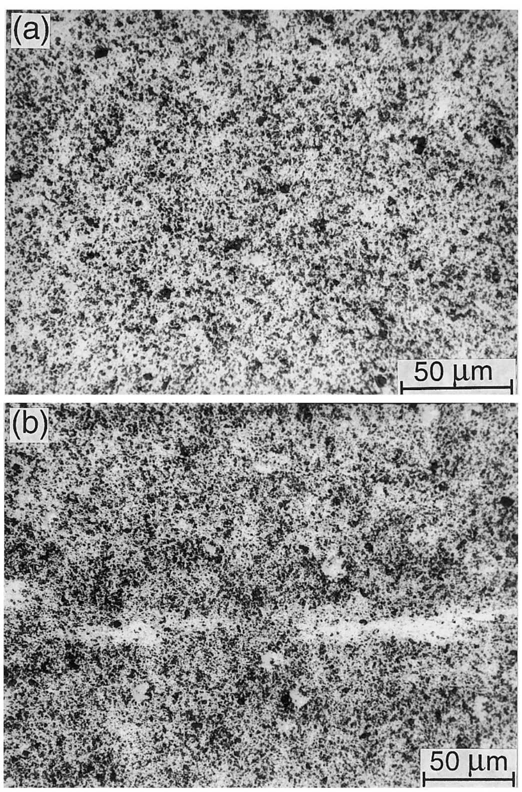

Fig. 4. Optical micrographs of a SiC_p(14.6 vol.%)/2024 extruded rod showing the distribution of SiC particles in (a) transverse and (b) longitudinal cross-sections (unetched).

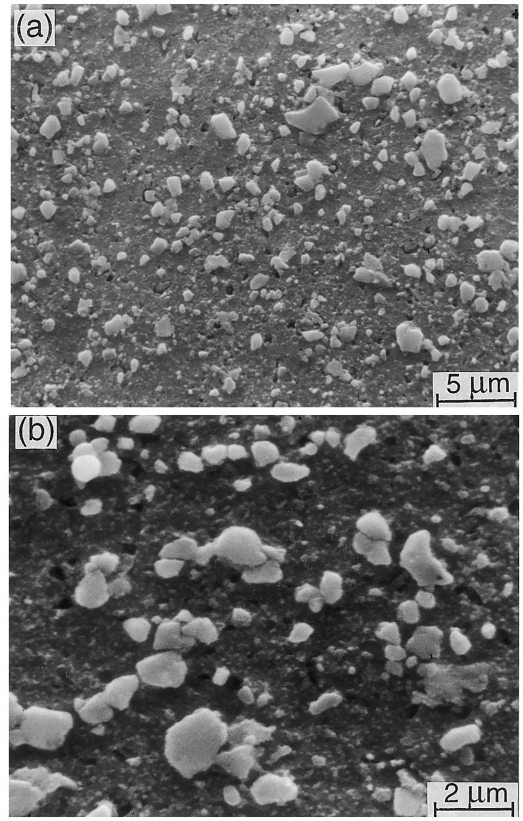

Fig. 5. SEM micrographs of a SiC_p(14.6 vol.%)/2024 extruded rod showing the aspect and distribution of SiC particles in (a) transverse and (b) longitudinal cross-sections (etched in 0.5% HF).

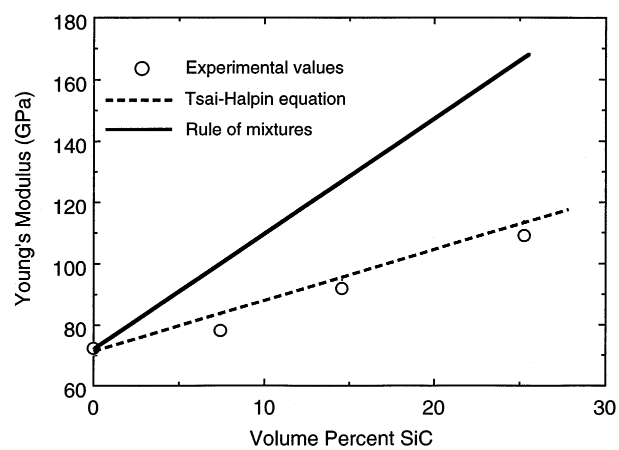

Fig. 6. Theoretically predicted elastic moduli for composites containing various volume fractions of SiC particles. The experimental values are also indicated.

Table 1
Mechanical properties of SiC_p/2024-T6 extruded rods and cast 2024-T6

Specimen	E (GPa)	Y.S. (MPa)	U.T.S. (MPa)	Elongation (%)
2024-T6 (cast)	72.4	393	476	10
2024-T6 (extruded powder)	73.8	402	485	10
SiC(7.4%)/2024-T6	77.9	453	514	5.2
SiC(14.6%)/2024-T6	91.7	496	571	4.4
SiC(25.3%)/2024-T6	109	595	665	2.4

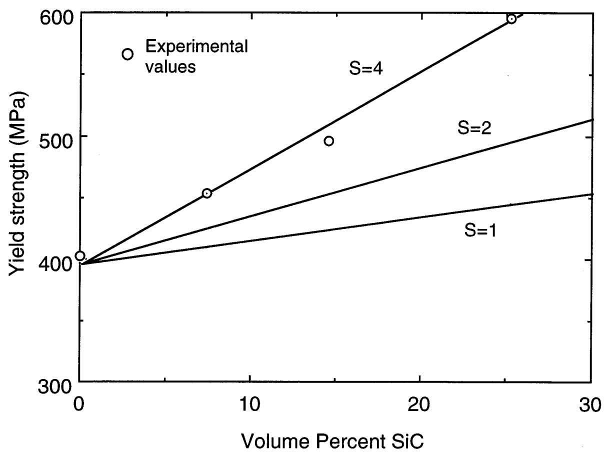

Fig. 7. Theoretically calculated yield strengths using different aspect ratios ($S = 1$, 2 and 4).

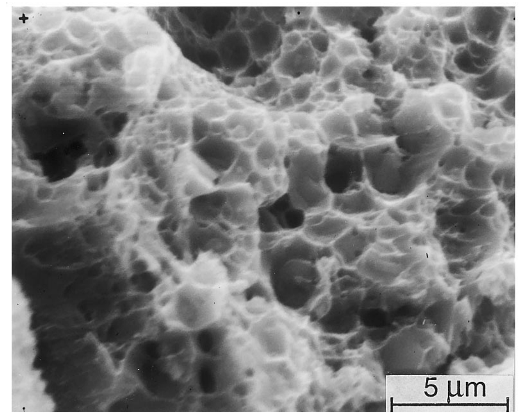

Fig. 8. SEM fractograph of 2024-T6 extruded rods tested in tension.

4. Conclusions

From the results of the present investigation, it can be concluded that SiC_p/2024 composite powders can be produced with a conventional low energy ball mill. Times required to produce a good composite powder are of course longer than in a high energy attritor but it is easy to handle and to maintain. Also, compared to the high energy attritor, the risk of contamination by the balls and the container material is significantly reduced in the case of low energy ball milling. The mechanical processing method is also very flexible and can be used to incorporate reinforcement particles of diverse nature in various metallic matrixes while avoiding damaging chemical reactions at the reinforcement/matrix interfaces.

The present study showed that the composite powders produced by mechanical processing in a low energy ball mill are adequate for making excellent composites. Composites containing up to 25 vol.% SiC_p exhibit superior mechanical properties and homogeneous distribution of reinforcement particles but their ductility decreases with the SiC_p content. The interface between 2024 matrix and SiC particles is very strong as revealed by fractography. In addition, the fractured surfaces show characteristics of a ductile rupture in the matrix at the microscopic level.

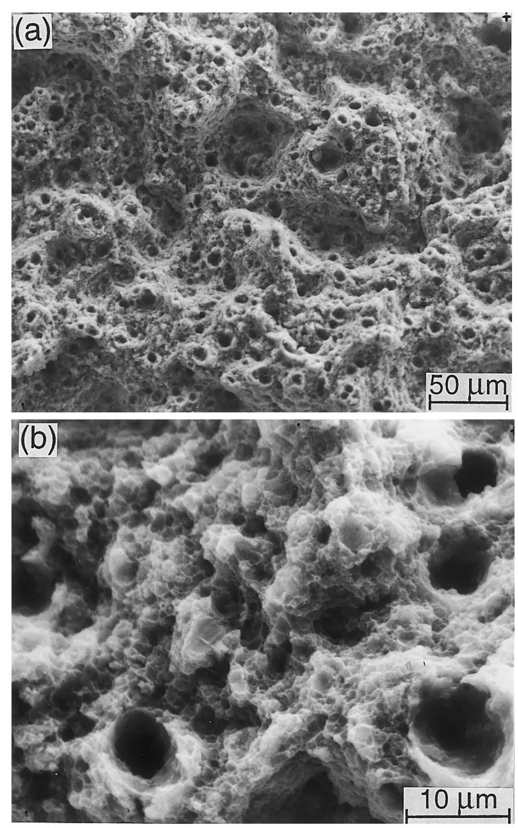

Fig. 9. (a) SEM fractograph of 7.5% SiC_p/2024-T6 extruded rods tested in tension. (b) Detailed aspect of craters and dimples.

The Young modulus of hot extruded composites was found in good agreement with that calculated from the Tsai–Halpin equation applied for particulate reinforcements [38]. The tensile yield strength of the composites was compared to the Nardone and Prewo model [39]. The experimental values of yield strength were fitted using an effective aspect ratio of 4, which is in accordance with other results previously published for similar composites produced by casting and by conventional powder metallurgy methods.

References

[1] S.J. Harris, Mater. Sci. Technol. 4 (1988) 231.
[2] H. Lagacé, D.J. Lloyd, Can. Metall. Quart. 28 (1989) 145.
[3] P. Rohatgi, J. Met. 43 (4) (1991) 10.
[4] N. Wang, Z. Wang, G.C. Weatherly, Metall. Trans. A 23 (1992) 1423.
[5] S.J. Swindlehurst, I.W. Hall, J. Mater. Sci. 29 (1994) 1075.
[6] M.D. Kulkarni, P.S. Robi, R.C. Prasad, P. Ramakrishnan, Scripta Metall. Mater. 31 (1994) 237.
[7] M. Gupta, M.K. Surappa, Key Eng. Mater. 104–107 (1995) 259.
[8] P.L. Liu, Z.G. Wang, W.L. Wang, Mater. Sci. Technol. 13 (1997) 667.
[9] M. Gupta, M.O. Lai, C.Y. Soo, Mater. Sci. Eng A210 (1996) 114.
[10] M. Gupta, F.A. Mohamed, E.J. Lavernia, Mater. Sci. Eng A144 (1991) 99.
[11] A. Mortensen, J.A. Cornie, M.C. Flemings, J. Met. 40 (1988) 12.
[12] D.L. McDanels, Metall. Trans. A 16A (1985) 1105.
[13] D. Dutta, C.G. Krishnadas Nair, K. Chattopadhyay, Key Eng. Mater. 29-31 (1989) 756.
[14] M. Manoharan, J.J. Lewandowski, Acta Metall. Mater. 38 (1990) 489.
[15] V.V. Bhanuprasad, R.B.V. Bhat, A.K. Kuruvilla, K.S. Prasad, A.B. Pandey, Y.R. Mahajan, Int. J. Powder Metall. 27 (1991) 227.
[16] M.P. Thomas, J.E. King, Mater. Sci. Technol. 9 (1993) 742.
[17] M.K. Jain, V.V. Bhanuprasad, S.V Kamat, A.B. Pandey, V.K. Varma, R.B.V. Bhat, Y.R. Mahajan, Int. J. Powder Metall. 29 (1993) 267.
[18] R.P. Schelleng, P.S. Gilman, A.P. Jatkar, J.S. Donachie, Powder Metall. Def. Technol. 6 (1985) 165.
[19] P.L. Davidson, Metall. Trans. A 18 (1987) 2115.
[20] R. Sundaresan, F.H. Froes, J. Metals 39 (8) (1987) 22.
[21] T.G. Nieh, C.M. McNally, J. Wadsworth, D.L. Yaney, P.S. Gilman, in: Y.-W. Kim, W.M. Griffith (Eds.), Dispersion Strengthened Aluminum Alloys, The Minerals, Metals and Materials Society, 1988, p. 681.
[22] S.J. Hong, P.W. Kao, Mater. Sci. Eng. A119 (1989) 153.
[23] F.H. Froes, J. Met. 41 (1) (1989) 25.
[24] S.J. Hong, P.W. Kao, Mater. Sci. Eng. A148 (1991) 189.
[25] S.J. Hong, P.W. Kao, C.P. Chang, Mater. Sci. Eng. A158 (1992) 195.
[26] J.F. Garneau, R. Angers, M.R. Krishnadev, L. Collins, Proc. CIM Conf., (1993) p. 27.
[27] E. Hochreiter, C. Kowanda, B. Ortner, J. Physique IV, Colloque C7 (Suppl. J. Phys.III), Vol. 3, November (1993) 1829.
[28] L. Lu, J.K.M. Kwok, M.O. Lai, Y.B. Liu, S.C. Lim, J. Mater. Proc. Technol. 37 (1993) 453.
[29] Y.B. Liu, J.K.M. Kwok, S.C. Lim, L. Lu, M.O. Lai, J. Mater. Proc. Technol. 37 (1993) 441.
[30] A. Bhaduri, V. Gopinathan, P. Ramakrishnan, G. Ede, A.P. Miodownik, Scripta Metall. Mater. 28 (1993) 907.
[31] J.-H. Lee, S.-J. Kim, C. Park, C.-H. Bae, J. Mater. Proc. Manuf. Sci. 4 (1995) 55.
[32] L. Lu, M.O. Lai, S. Zhang, Key Eng. Mater. 104–107 (1995) 111.
[33] A. Bhaduri, V. Gopinathan, P. Ramakrishnan, A.P. Miodownik, Mater. Sci. Eng. A221 (1996) 94.
[34] L. Lu, M.O. Lai, S.H. Yap, Mater. Sci. Technol. 13 (1997) 192.
[35] Annual Handbook of ASTM Standards, Volume 2.02, Section 2: Aluminum and magnesium alloys, 1997.
[36] D.L. Davidson, Metall. Trans. A 22 (1991) 113.
[37] J.J. Lewandowski, C. Liu, Mater. Sci. Eng. 107 (1989) 241.
[38] J.C. Halpin, Primer on Composite Materials Analysis, Technomic Publ. Co., 2nd edition., Lancaster-Basel, 1992.
[39] V.C. Nardone, K.M. Prewo, Scripta Metall. 20 (1986) 43.
[40] R.J. Arsenault, R.M. Fisher, Scripta Metall. 17 (1983) 67.
[41] M.B. House, K.C. Meinert, R.B. Bhagat, J. Met. 43 (8) (1991) 24.
[42] T. Christman, S. Suresh, Acta Mater. 36 (1988) 1691.